π^- +p ELASTIC SCATTERING NEAR .893 AND 1.03 BeV/c

by

William Redin Dawes, Jr.

A Dissertation Submitted to the Faculty of the

DEPARTMENT OF PHYSICS

In Partial Fulfillment of the Requirements
For the Degree of

DOCTOR OF PHILOSOPHY

In the Graduate College

THE UNIVERSITY OF ARIZONA

1968

THE UNIVERSITY OF ARIZONA

GRADUATE COLLEGE

I hereby recommend that this dissertation prepared under my direction by William Redin Dawes, Jr.

entitled $\pi^- + p$ Elastic Scattering Near .893 and 1.03 BeV/c

be accepted as fulfilling the dissertation requirement of the degree of Doctor of Philosophy

Theodore Bowen — Dissertation Director

12/19/67 — Date

After inspection of the final copy of the dissertation, the following members of the Final Examination Committee concur in its approval and recommend its acceptance:*

Edgar W. Jenkins

Joseph J. Veillerman

Glenn Mehlman

Chang-Yun Fan

*This approval and acceptance is contingent on the candidate's adequate performance and defense of this dissertation at the final oral examination. The inclusion of this sheet bound into the library copy of the dissertation is evidence of satisfactory performance at the final examination.

STATEMENT BY AUTHOR

This dissertation has been submitted in partial fulfillment of requirements for an advanced degree at The University of Arizona and is deposited in the University Library to be made available to borrowers under rules of the Library.

Brief quotations from this dissertation are allowable without special permission, provided that accurate acknowledgment of source is made. Requests for permission for extended quotation from or reproduction of this manuscript in whole or in part may be granted by the head of the major department or the Dean of the Graduate College when in his judgment the proposed use of the material is in the interests of scholarship. In all other instances, however, permission must be obtained from the author.

SIGNED: Wm R. Hamer, Jr.

ACKNOWLEDGMENTS

I wish to express my appreciation to Professor Theodore Bowen who initiated and actively participated in all aspects of this experiment. I wish to also thank Dr. D. A. De Lise, Dr. E. W. Jenkins, Dr. R. M. Kalbach, Dr. E. Malamud, Dr. G. B. Yodh, J. J. Jones, D. Petersen, R. Ferry, and our scanners for their help in completing this work.

To my wife, Jeanne, I give the greatest thanks for her many sacrifices, encouragement and understanding during the difficult times leading to the completion of this dissertation.

TABLE OF CONTENTS

LIST OF ILLUSTRATIONS

ABSTRACT

Fluctuations observed in the cross sections of low energy nuclear scattering experiments have been successfully explained by assuming the reaction is dominated by a statistical process. This experiment examined the $\pi^- + p$ elastic scattering reaction at five incident pion momenta ranging from 1.02 to 1.06 BeV/c to determine if there were any fluctuations that could be explained by a statistical process. Within the errors of the experiment, no fluctuations of this nature were observed.

Spark chambers were used to determine the differential cross section over the angular range of $-.2 < \cos \theta^* < .8$ where θ^* is the center-of-mass scattering angle. Of the 1,800 elastic scattering events measured at a nominal momentum of 1.03 BeV/c, 1,030 had their incident pion momenta determined to .1%. Two hundred occurred in the angular region of $.05 < \cos \theta^* < .45$, which is outside the forward diffraction peak and in a region where corrections due to geometrical biases were not required. These events were grouped into five momentum bins and examined for fluctuations over small changes in incident pion momenta. Six hundred $\pi^- + p$ elastic scattering events were measured at .893 BeV/c to determine geometrical biases and to confirm the normalizations and corrections used.

1. INTRODUCTION

In recent years, rapid fluctuations observed in nuclear reactions involving excitation energies of 12-20 Mev have been successfully explained by the fluctuation theory of Ericson.[1] The theory assumes that the matrix elements of the compound nucleus are randomly distributed with respect to phase and amplitude.[2] Let α, i, and α' represent the initial, intermediate, and final state, respectively, and S_α and $S_{\alpha'}$ represent the scattering matrix for the initial and final states, with f(E, Ei) the probability amplitude of exciting the intermediate states. Then we can write

$$\sigma_{\alpha\alpha'}(E) = \left|\Sigma < \alpha|\ S_\alpha\ |i > f(E, Ei) < i|\ S_{\alpha'}\ |\ \alpha' >\right|^2$$

Both $< \alpha\ |\ S_\alpha\ |i >$ and $< i|\ S_{\alpha'}\ |\alpha' >$ are assumed to have random phases. If we examine a different final state under the same conditions, the transition elements will be randomly independent and $\sigma_{\alpha\alpha'}(E)$ will exhibit fluctuations. This experiment was performed to ascertain whether similar fluctuations occurred in high energy interactions.

The π^- +p elastic scattering reaction was investigated at incident pion momenta of .893 BeV/c and 1.03 BeV/c with a 2% spread. The data at .893 BeV/c was used as a check on our normalizations, while the 1.03 BeV/c data was divided into five momentum bins to investigate the fluctuations. The experiment should see the fluctuations if there is a state in the π^- +p system whose width is in the range of 3 to

20 Mev and if the fluctuations do indeed occur in the energy range of our experiment.

The π^- +p elastic scattering process was examined by spark chambers whose geometry allowed us to investigate the center-of-mass scattering angular region of 35° to 105°. The events were analyzed by the University of Arizona fitting and bookkeeping package of PREPARE, GEOKIN, STRAW, and SUMX. The results indicated that under our experimental conditions, the fluctuations proposed by Ericson do not occur.

Allaby, et al., investigated proton-proton elastic scattering at 16.9 BeV/c for Ericson fluctuations in the angular distribution but did not observe any within their experimental errors.[3]

2. APPARATUS

The experimental apparatus was originally designed to examine the $\pi^- + p \rightarrow \Lambda^\circ + K^\circ$ reaction at the Berkeley Bevatron. Because of the incident pion fluxes used, the $\pi^- + p \rightarrow \Lambda^\circ + K^\circ$ reaction occurred about once for every 250 milliseconds of beam spill at 1.03 BeV/c. It was possible, therefore, to use the last 50 - 30 milliseconds of beam spill to examine the $\pi^- + p$ elastic scattering reaction without significant loss of events in the primary experiment. At 1.03 BeV/c, at least one elastic scattering event occurred per 50 milliseconds of beam spill.

The pi minus mesons were produced by flipping a 1" x $\frac{1}{4}$" x $\frac{1}{4}$" movable platinum target into the Bevatron's circulating proton beam. The movable target was used to allow adjustments in the flux and in the central momentum of the pi minus mesons. The beam was designed to obtain approximately 20,000 pi minus mesons per Bevatron pulse with an 800 millisecond beam spill at any laboratory momentum from .890 BeV/c to 1.20 BeV/c.

The beam layout is shown in Figure 1. The C magnet bent the negatively charged particles produced inside the Bevatron into the first triplet quadrupole, Q1. The collimators K1 and K2, located just behind Q1 and at the vertical and horizontal focus of Q1, respectively, defined the particle path in the beam pipe. The bending magnet, H, selected the desired central momentum of the particles which were then

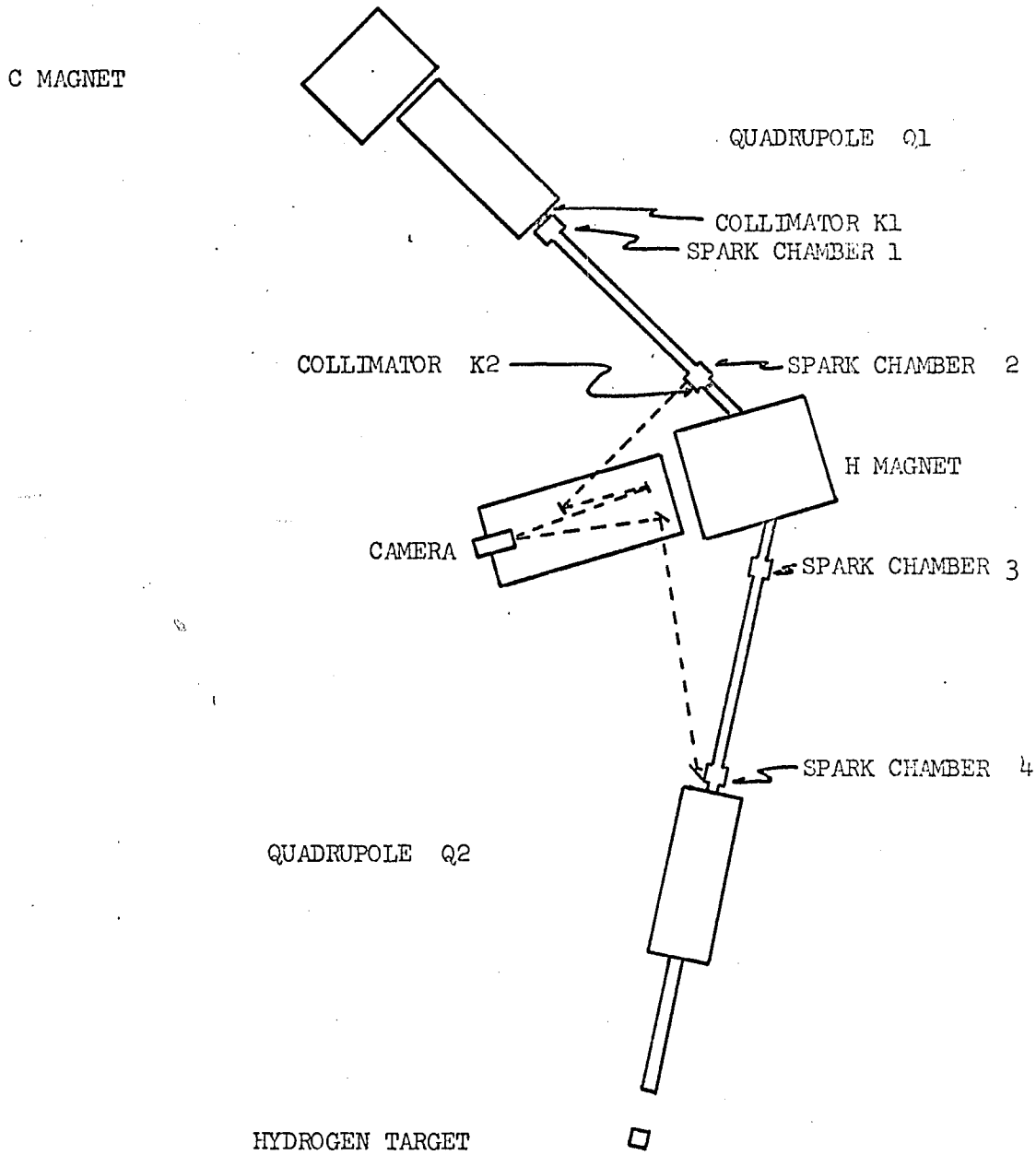

FIGURE 1 BEAM LAYOUT

The light paths for spark chambers 1 and 3 are the same as those for 4 and 2 respectively.

focused on the 1" thick liquid hydrogen target by the second triplet quadrupole, Q2.

The beam contamination was due to electrons from conversion of gamma rays in the platinum target and to muons from the decay of pi's in the beam transport system. The amount of contamination was estimated by observing beam tracks in the range chamber, i.e., tracks of particles that did not interact in the hydrogen target. The electron contamination was determined by noting the percentage of beam tracks that were accompanied by an electron shower. The electron contamination was 9% ± 1%. The graduated thickness of absorber in the range chamber was used to determine the muon contamination. The beam tracks not accompanied by an electron shower were placed in two categories, those that stopped, interacted or suffered a large angle scattering in the range chamber, and those that traversed the range chamber. The beam tracks in the first category must be the negative pions. An extrapolation of the number of beam tracks from this category, versus the amount of material traversed before stopping yields the number of pions expected in the second category. The difference between the number expected and the number found was attributed to the muon contamination. The muon contamination was 25% ± 2.5 % . The total beam contamination was 34% ± 2.9% and was, within our errors, independent of our incident momenta.

The four spark chambers, 1-4, and the beam transport system (Fig. 1) shared a common atmosphere, which was pure helium gas at 250 torr. Spark chambers 2 and 3 each had a single 1" gap constructed with

0.001" beryllium foils to minimize the multiple coulomb scattering. Spark chambers 1 and 4 each had two 1" gaps constructed with 0.001" aluminum foil. These four chambers were used to determine the entrance and exit points of a particle upon traversing the H magnet's field. The beam pipe sections between spark chambers 1 and 2 and between 3 and 4 were magnetically shielded to keep their interiors field free. The H magnet's field was measured at five current settings to an accuracy of two gauss. During the experiment, the H magnet's current was monitored by a five place potentiometer and by a four place digital voltmeter. The H magnet's field was also monitored by a nuclear magnetic resonance probe.

Figure 1 also illustrates the photographic setup for the beam spectrometer. The optical paths were chosen such that spark chambers 1-4 were optically equidistant from the camera. Each frame contained the horizontal and vertical projections of the sparks in all four spark chambers, as well as the digital voltmeter reading of the H magnet's current and the beam event register number. A second event register, synchronous with the beam event register, was photographed by a second camera observing the interactions and was used to correlate the incident pion momentum with each interaction. These registers were frequently checked during the experiment to insure their synchronization. A double frame 35 mm camera using a 300 mm lens at f/5 with Tri-X film was used to photograph the spectrometer chambers.

The central momenta selected during the experiment ranged from .890 to 1.2 BeV/c. The collimators restricted each momentum bite to 2%

at half maximum. For the elastic scattering experiment, only the data at .893 and 1.03 BeV/c were analyzed. One half of the data was taken at 1.03 BeV/c, corresponding to 8,000 elastic scattering events, with 13% of the data taken at .893 BeV/c. The data taken at each of the other momenta was less than 8% of the total data and insufficient to analyze elastic scattering. Figure 2 shows the beam momentum profiles for 1.03 BeV/c, and indicates that we were actually at 1.04 BeV/c. The momentum determination is discussed in the Data Analysis section.

Figure 3 illustrates the arrangement of spark chambers, target, and scintillation detectors used to examine the $\pi^- + p$ elastic scattering process. The beam was defined by the scintillation detectors 1 and 3 in coincidence and 2 and 4 in anticoincidence. These requirements restricted the acceptable incident pions to a circular region with a 1.0" diameter that was centered on the 3" diameter hydrogen target. The final logic requirement was that there be an anticoincidence in scintillation detector 7. The solid angle subtended by this scintillator with respect to the target caused only those elastic scattering events where both particles traversed spark chamber 6 to be accepted. Scintillator 7 also restricted the triggering requirements to those events where the incident pion had interacted. These logic requirements caused triggering on many non-elastic events which had to be eliminated either by scanning or by the kinematic fitting. Scintillation detectors 5 and 6 were used only in the $\pi^- + p \rightarrow \Lambda^\circ + K^\circ$ experiment.

Spark chamber 5, the beam chamber, consisted of eight 5" x 5" x .001" aluminum foil plates making two pairs of .375" gaps with 5"

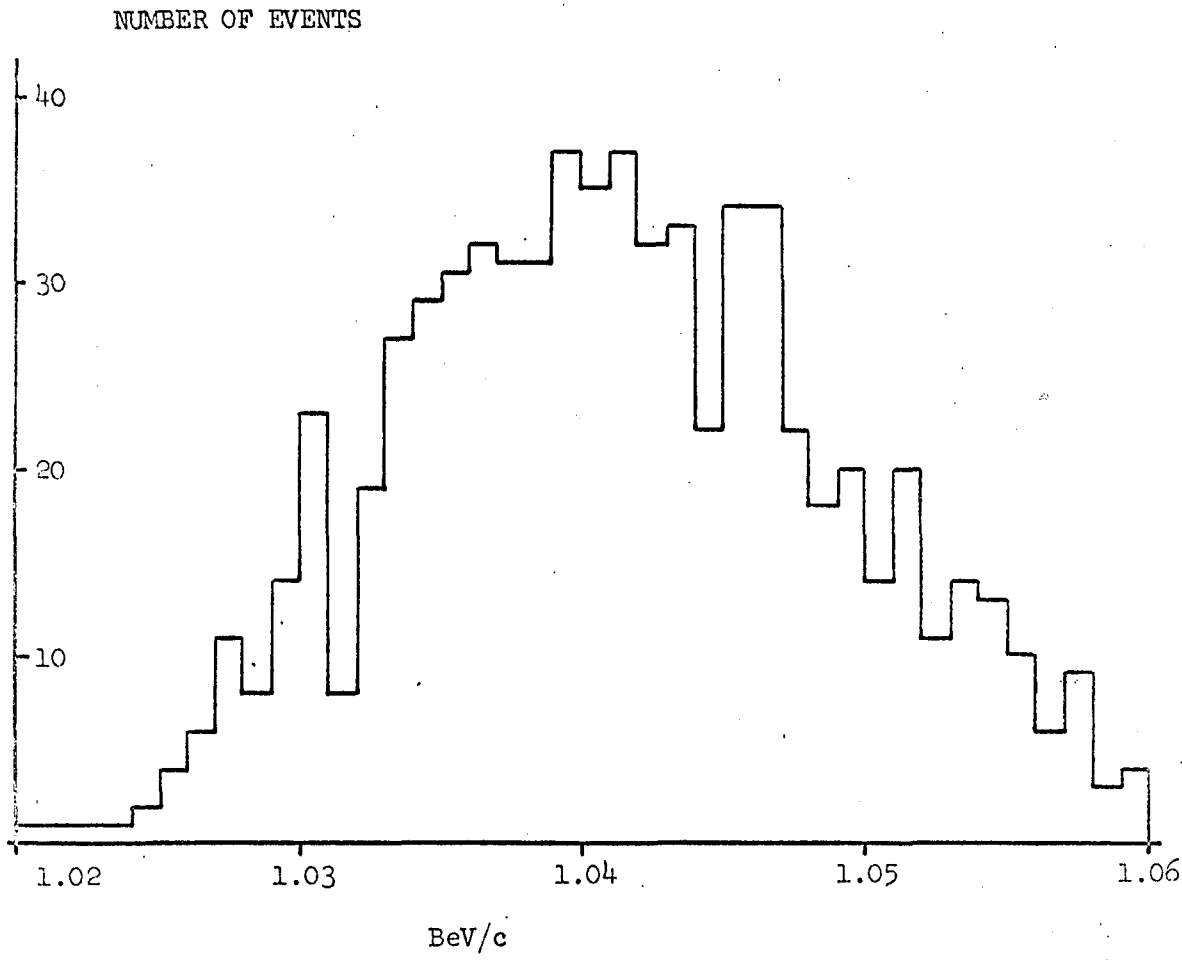

FIGURE 2 BEAM PROFILE FOR 1.03 BeV/c

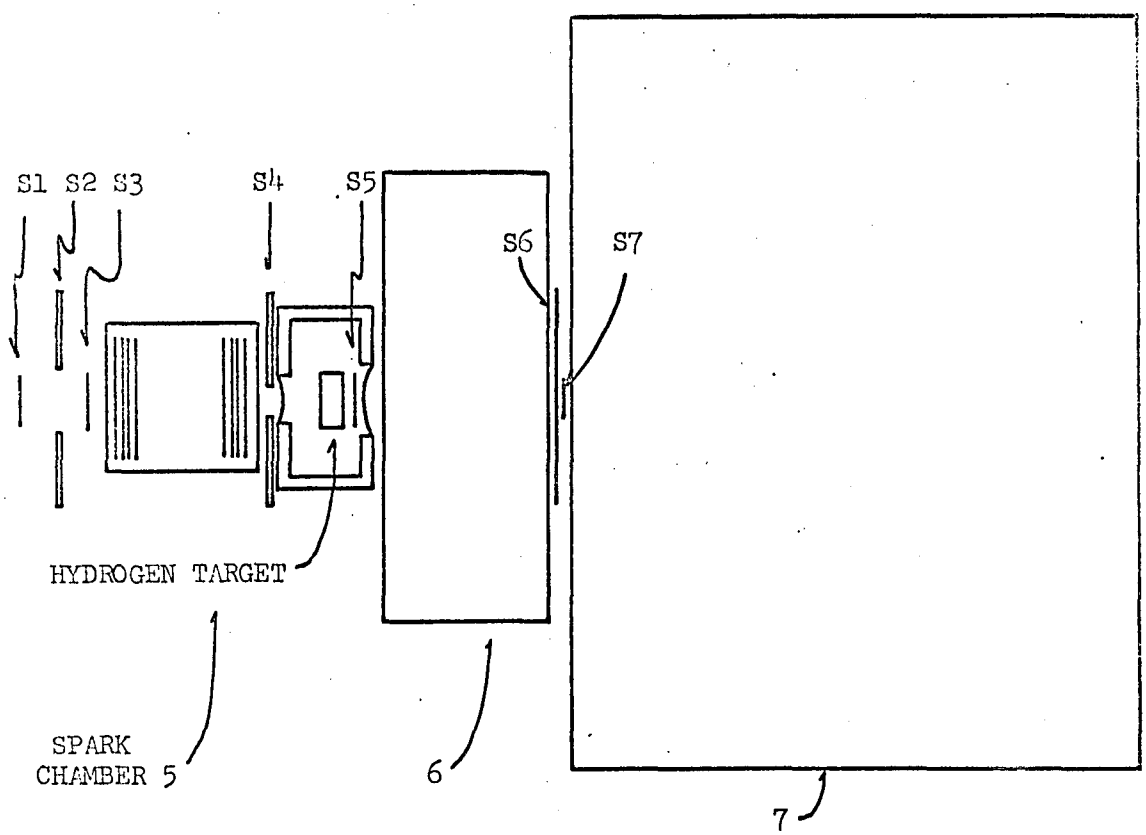

FIGURE 3 ARRANGEMENT OF TARGET, SCINTILLATORS, AND SPARK CHAMBERS

between the two pairs; it was used to determine the direction of the incident pion. Spark chamber 6, the event chamber, consisted of sixteen 2' x 2' x .001" aluminum foil plates, making eight .375" gaps, and was used to determine the direction of particles leaving the target. The aluminum foil was used in the beam and event chambers to minimize the multiple coulomb scattering of the observed particles. The 106 gm/cm^2 range chamber, spark chamber 7, used graduated thicknesses of aluminum absorber to determine the ranges of observed particles. The graduations were chosen such that the percentage of error in the momentum determined by the range information would remain constant. About 1 gm/cm^2 was traversed by the particles entering spark chamber 7 from the hydrogen target. The absorber was measured, weighed, and then inserted between 3' x 3' x .5" sealed spark chamber modules.

Two 45° mirrors, mounted on the same frame, were located underneath spark chambers 5, 6, and 7. The smaller mirror projected the image from the first two gaps of spark chamber 5, and the larger mirror projected the remaining image from the gaps of spark chambers 5, 6, and 7. Two mirrors were required because of obstructions due to the supporting framework of the spark chamber assembly. Two 30 foot focal length field lenses, mounted in the vertical plane, were used to permit simultaneously viewing parallel to all of the spark chamber gaps. Each photograph of an event contained the date and time of the experiment, the roll number of the film, and a register number. A double frame 35 mm camera using a 135 mm lens at f/8 with Tri-X film was used to record the events.

Figure 4 is a block diagram of the electronics associated with the π^- +p elastic scattering experiment. The signals from S1 and S3, two of the beam event scintillators, were each fed into a University of Arizona fast discriminator whose output was connected to a coincidence input channel of a University of Arizona coincidence circuit. The signals from S2 and S4 were amplified, mixed and then connected into the anticoincidence channel of the coincidence circuit, C1. This coincidence circuit was gated to fire only during the beam spill. One output of C1 went into a fast discriminator that was gated to the beam spill of the π^- +p elastic scattering experiment and to the camera control. The camera control gate was used to prevent any interaction from triggering the apparatus during the camera cycle time of 100 milliseconds. The output from the fast discriminator went to a scaler which recorded the incident pion flux for the π^- +p elastic scattering process.

The other output from C1 was connected to a coincidence input of a second coincidence circuit, C2. The signal from scintillator S7 was amplified and then connected to the anticoincidence input of C2. C2 was gated to the beam spill of the π^- +p elastic scattering experiment and to the camera control. One of the outputs from C2 went to a scaler that recorded the number of counts and to an SCR circuit which triggered the "B" nixie light appearing on the photograph of an event. The other output went into a fast discriminator whose output triggered the camera and spark chambers. The logic requirement for an elastic scattering event, therefore, was S1, $\overline{S2}$, S3, $\overline{S4}$, and $\overline{S7}$.

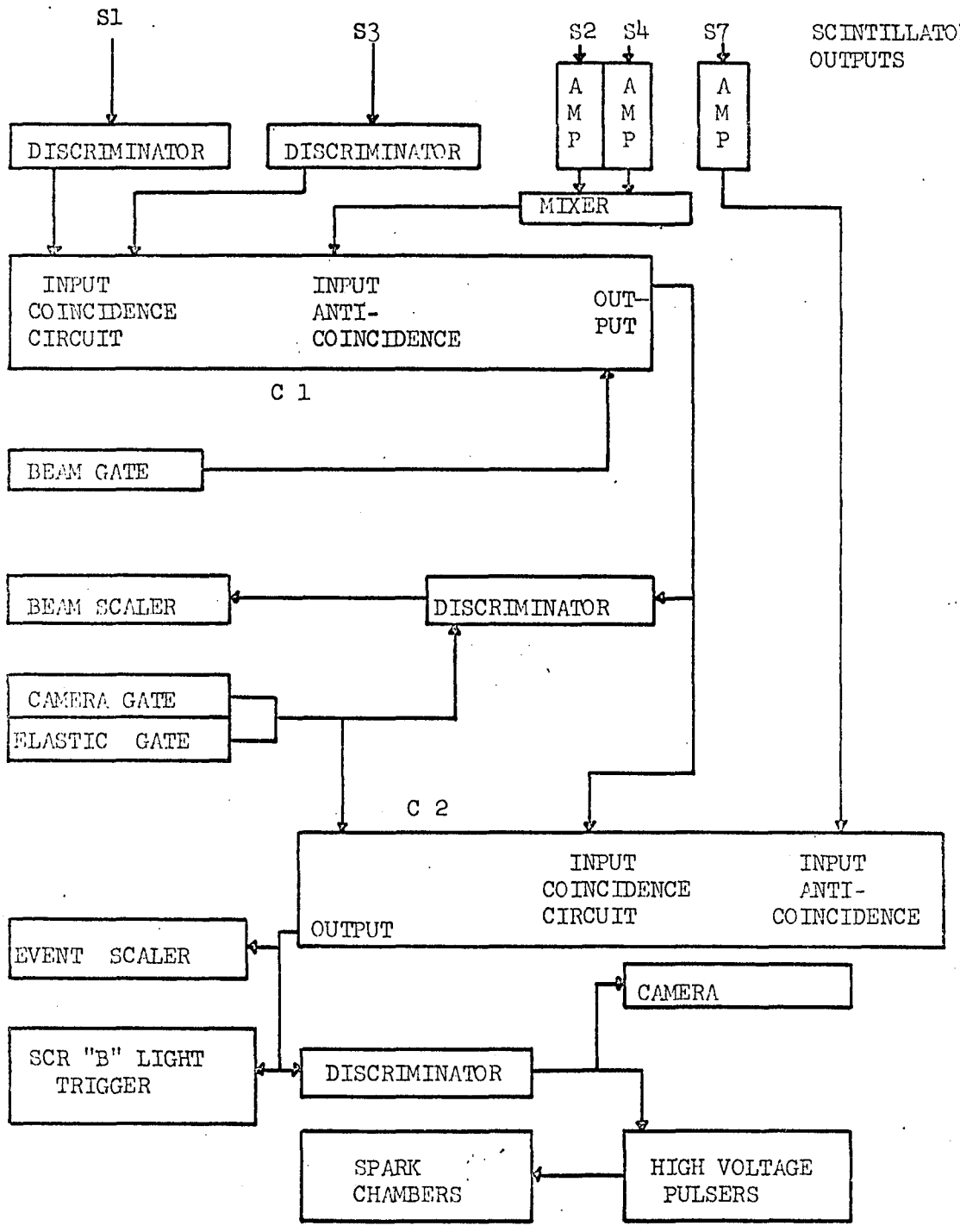

FIGURE 4 BLOCK DIAGRAM OF THE ELECTRONIC APPARATUS

The spark chambers for the pion spectrometer were fired by a high voltage spark gap pulser based on a design from Argonne National Laboratory. An avalance transistor and two fast-switching tubes amplified the initial input trigger pulse to 7 kilovolts, which then connected 17 kilovolts across the spectrometer spark chambers by means of a spark gap switch.

The beam spark chambers and event spark chambers, spark chambers 5 and 6, were pulsed by two 5C22 thyratron pulsing circuits. These were triggered by the EFP-60 and 3C45 circuits whose pulses were initiated by the trigger pulse from C2. The range spark chambers received their high voltage pulses from spark gap switches whose trigger pulses were activated by another Argonne high voltage pulser.

3. DATA ANALYSIS

The incident pion momentum was determined by the beam spectrometer system which is illustrated in Figure 1. Spark chambers 1 and 2 defined the particle's trajectory as it entered the magnetic field of the H magnet and spark chambers 3 and 4 defined the exit trajectory. Orthogonal projections of each spark were recorded by the photographic system to facilitate the fitting in two separate planes. The crucial fit was in the plane perpendicular to the magnet field, the horizontal plane; since the fit in the vertical plane involved a second order focusing effect of the magnetic field, it gave a check that all sparks were due to the same particle.

The magnet gap was 60" x 18" x 4" and the following orthogonal left-handed coordinate system was used to describe its field. The x axis was parallel to all four sides and down the 60" length. The y axis was perpendicular to the 4" x 60" wall. The strongest component of the field was along the z direction. The magnetic field was measured at five different currents in a 1" square grid in the x-y plane for three values of z to an accuracy of 2 gauss. The fiducials for the four beam spark chambers were also defined in terms of the magnet's coordinate system.

The z component of the H magnet's field, B_z, within the area traversed by the incident pions, was first expressed by a third order

polynomial in current over the current range used in the experiment,

$$B_z = A_0(x,y,z) + A_1(x,y,z)I + A_2(x,y,z)I^2 + A_3(x,y,z)I^3 \ .$$

Each coefficient of this polynomial was then expressed as a third order polynomial in y,

$$A_i = B_0{}^i(x,z) + B_1{}^i(x,z)y + B_2{}^i(x,z)y^2 + B_3{}^i(x,z)y^3 \ . \quad i = 0, 1, 2, 3.$$

Finally, each of these coefficients were defined by a second order expansion in z,

$$B_i{}^j = C_0{}^{ij}(x) + C_1{}^{ij}(x)z + C_2{}^{ij}(x)z^2 \ . \qquad \begin{matrix} i = 0, 1, 2, 3 \\ j = 0, 1, 2, 3 \end{matrix}$$

The final expression for B_z, therefore, involved forty-eight coefficients.

Since the expression for the field was determined for a source free region, we can write the general expression for the scaler potential, ϕ, as

$\phi = - \int B_z \cdot dz + A(x,y)$, where $A(x,y)$ is an arbitrary function of x and y. Then,

$$B_x = - \frac{\partial \phi}{\partial x} \ , \qquad B_y = - \frac{\partial \phi}{\partial y} \ .$$

Because of the symmetry of the magnet with respect to the origin of coordinates at its center, there can be no contribution to B_x or B_y by a z independent term in ϕ. Therefore, $A(x,y)$ is zero and B_x and B_y can be obtained from the following expressions:

$$B_x = \frac{\partial}{\partial x} \int_{-.8}^{.8} B_z \cdot dz \qquad \text{and} \qquad B_y = \frac{\partial}{\partial y} \int_{-.8}^{.8} B_z \cdot dz \ .$$

These components of the magnetic field are needed to determine the second order vertical focusing.

The fitting by least squares of momentum, magnetic field, and spark position was possible only if at least three valid track locations were known. 35% of all triggered spectrometer events had less than three valid track locations, primarily because of the effects of multiple tracks in chambers 1 and 2 where the flux was highest. The calculated momentum of fits using three track locations agreed with fits using four track locations to within .03%. The absolute calibration of the beam fitting was done by comparing fitted values of momentum from the $\pi^- + p \rightarrow \Lambda^\circ + K^\circ$ reaction.

The logic indicator light, a nixie tube, flashed an "A" or a "B" simultaneously with the spark chamber triggering to indicate whether the logic requirements were for $\pi^- + p \rightarrow \Lambda^\circ + K^\circ$ or for $\pi^- + p \rightarrow \pi^- + p$ respectively. The first measuring criteria for the elastic scattering events therefore was a "B" logic indication. Two other requirements for measurement were that the apparent vertex be near the known location of the hydrogen target, indicated by a fiducial and that the beam track from chamber 5 extrapolate between both tracks in each view. The second requirement eliminated many decay and non-hydrogen background events and the final requirement eliminated the obviously noncoplanar events. Even with these criteria, approximately 75% of the measured 1.03 BeV/c events were non-elastic background events.

The scanning efficiencies were calculated by scanning all of the film twice. Each event found in the double scan was placed into

one of three categories. The number of events in each are:

1) N_{ab}, events found by scanner A and scanner B;

2) N_a, events found by scanner A only; and

3) N_b, events found by scanner B only.

The scanning efficiencies for scanner A, e_a, and scanner B, e_b, then are

$$e_a = N_{AB}/(N_B + N_{AB}) \quad \text{and} \quad e_b = N_{AB}/(N_A + N_{AB}) .$$

The combined scanning efficiency for an event to be found by scanner A or scanner B is

$$e_{a \text{ or } b} = (N_A + N_B + N_{AB})\, N_{AB} \Big/ (N_A + N_{AB})\,(N_B + N_{AB}) .$$

These relations are true assuming that the two scans are statistically independent. The most probable value for the total number of events is

$$N_o = (N_A + N_{AB})\,(N_B + N_{AB}) \Big/ N_{AB}$$

where $N_o = N_A + N_B + N_{AB}$ + events missed by both scanners. Using the treatment of Abrams,[4] the uncertainty of N_o due to the statistical fluctuations of N_A, N_B, and N_{AB} is given by

$$(\delta N_o)_{sc} = \sqrt{\frac{N_o\,(1 - e_a)(1 - e_b)}{e_a\, e_b}} .$$

Assuming a Poisson distribution for N_o, $\delta N_o = \sqrt{(\delta N_o)_{sc}^2 + N_o}$. If the value of $\sqrt{\frac{(1 - e_a)(1 - e_b)}{e_a\, e_b}}$ is small compared to unity, then the uncertainty in N_o will be approximately $\sqrt{N_o}$. This condition is equivalent to a double scanning efficiency of 95%. All rolls having a double scanning efficiency of less than 95% were scanned a third time to

minimize the errors due to scanning inefficiencies. The total scanning efficiency for the experiment was 98%.

The events were first scanned and measured on a Nuclear Research Instruments measuring machine. The reticle pattern projected on the screen was a rotatable arrow with a small cross-bar. The coordinate system of the machine used the angle of the arrow and the x-y position of the intersection of the arrow and the cross-bar. The measuring procedure was to center the intersection point on the first spark of a track and align the arrow along the remaining sparks of the track. Activating the recording sequence of the measuring machine transferred the x-y coordinate position and the arrow's angle, θ, to a punched card. The machine least count error in the cartesian coordinates was 1 micron, and on the angle, .006 radians.

To determine distortions in the optical system, two 3' x 6' grids with a 1/2" x 1/2" pattern were placed directly over the sides of the spark chambers viewed by the event camera. Selected points on the grid were then measured by the measuring machine and reconstructed. Approximately 100 beam tracks, tracks of particles that traversed all three spark chambers (5, 6, and 7) without interacting, were measured at three points in both projected views and their slopes and intercepts were compared. No distortions in the field lenses were found, but it was determined that the y magnification was 1.023 times greater than the x magnification, and that the z magnification was 1.020 times greater than the x magnification.

The three sets of fiducials were surveyed both before and after the conclusion of the experiments to an accuracy of 1/16". The first

set defined the x-y coordinates, the second set defined the x-z coordinates viewed by the larger of the two 45° mirrors, while the third set defined the x-z coordinates for the smaller 45° mirror. The fiducial coordinates were adjusted slightly so that sparks measured in both views had the same x-position, the x axis being common to both views. The third fiducial set was adjusted such that the coordinates of beam tracks measured in spark chamber 5 were on a line whose slope and intercept were determined by measurement in spark chamber 6, using the second fiducial set. The adjustments on the fiducials were of the order of the fiducial errors.

The IBM cards containing the punched output from the film measuring machine were analyzed by PREPARE, a program designed to transform the data into a format applicable to fitting. PREPARE rejected all events where:

1) the card format was incorrectly made out;

2) the calculated magnification was outside the acceptable limits of ± 2%;

3) the angle of any track was in an improper quadrant; and

4) the data cards were mixed up.

These rejected events were remeasured and submitted again to PREPARE.

The film measuring machine defined each track by an x-y or an x-z coordinate and an angle, θ. Those events not rejected were converted by PREPARE such that the tracks were defined by a slope and an intercept. The errors of these slopes and intercepts as well as their correlations were also calculated. This calculation required a knowledge of the variances of x, y, z, and θ.

The variances of the slope and the intercept as well as their correlations are proportional to $\sigma_y^2 + a^2\sigma_x^2$, where a is the slope of the track and σ_x, σ_y are the variances of x and y measurements respectively. In order to estimate σ_x and σ_y, three points were measured on each of approximately 600 tracks, about half of which had slopes greater than 1. Each group of three points was then fitted to a straight line using the method of least squares and placed into one of two groups depending upon the value of its slope. The chi-squares of the first group, containing those tracks whose slopes were less than .2, depend primarily upon the value of σ_y^2 for the experiment. Similarly, the chi-square distribution of the second group, containing those tracks whose slopes were greater than 1, was used to determine the proper value of σ_x^2. As a check, the chi-square distribution for approximately 400 fitted events, with no restrictions on their slopes, was plotted and found to have the predicted distribution. The values determined for the variances were $\sigma_y = \sigma_z = .018"$, and $\sigma_x = .035"$. A similar technique was used to ascertain the variance of θ, which was $\sigma_\theta = .008$ radians.

These errors represent the errors of measuring points along a track determined by a series of sparks. The incident pion track was measured in this manner. The measuring procedure for event tracks, however, was to center the reticle pivot position on the first spark of a track and then to align the reticle along the track. While this method was faster than measuring points, it had a greater error. The new errors were again determined by requiring a correct chi-square distribution, this time from fitting the coplanarity of known elastic

scattering events. The final errors used by the following programs were σ_x=.07", $\sigma_z = \sigma_y$ = .03", and σ_θ= .008 radians.

The output of PREPARE was the slope intercept, slope error, intercept error, and correlation for each of the six tracks defining an elastic scattering event. The range, in gm/cm^2, of the final state particles and the nominal incident pion momentum was also part of the output. The output of PREPARE was then processed by the fitting program GEO-KIN III.

The fitting was done by the standard method of least squares discussed by Böch, and was done in two steps.[5] The first phase of the program fitted the six tracks, the two projections of the three tracks associated with the event, to a common vertex and simultaneously required that they be coplanar. The requirements for a good fit were rather lenient; the constraint equations had to be satisfied to .001", and the chi-square of the fit had to be within the 99% confidence level. Events failed for either one of three reasons:

1) the fitting would not converge; or

2) the chi-square of the event exceeded the 99% confidence level; or

3) the interaction did not occur in the target or in the Λ° K° experiment scintillator region directly behind the target.

Events satisfying the requirements for a good fit were then converted into a three dimensional format by converting the fitted slopes and intercepts into direction cosines and intercepts. These events were specified as either target events or scintillator events, and then were allowed to pass into the second phase of the fitting.

The passed events were then fitted to the constraints of energy and momentum conservation for elastic scattering events. The criteria for an acceptable fit were satisfaction of the constraint equations to 1 MeV/c and a chi-square within the 99% confidence level. Events satisfying the kinematics fit had their geometrical and kinematical parameters, as determined by the fitting program, stored on a magnetic tape if the fitted momenta were equal to or greater than the momenta determined from the range information.

A Monte Carlo program was used to ascertain the reliability of GEO-KIN III. For both phases of the fitting, the chi-square distribution agreed with the theoretical distribution. The Monte Carlo program was also used to obtain an estimate of the variance of $\cos \theta^*$. A histogram was plotted of the difference between the fitted value of $\cos \theta^*$ used by Monte Carlo before the errors were introduced. The full width at half maximum was .03, which was in agreement with the errors calculated by the fitting program. The reverse-pion ambiguity, mistaking the pion for the proton was also investigated by use of the Monte Carlo program. At 1.03 BeV/c this ambiguity occurs near $\cos \theta^* = +.22$, where the pion and proton laboratory angles are nearly equal. In the cases where the best kinematical fit was obtained when the pion was mistaken for the proton, the difference in the true value of $\cos \theta^*$ and the fitted value was within the .03 error associated with $\cos \theta^*$.

The fitted events for each particular momentum were placed in histograms of $d\sigma/d\Omega$ versus $\cos \theta^*$. The Legendre polynomials were then fitted to the histograms by STRAW. Since the experiment investigated

the π^- +p elastic scattering process only in the center-of-mass scattering angular region of 35° to 105°, the argument of the Legendre polynomials used by STRAW was transformed so that they would be orthogonal over this angular range. This was done by defining $x = 2 \cos \theta^* - .6$ so that x would range from +1 to -1 as $\cos \theta^*$ ranges from +.8 to -.2 .

STRAW minimized

$$\chi^2 = \sum_{i=o}^{n} (N_o{}^i - N^i)^2 / \sigma_i{}^2$$

where N was the number of bins in the histogram, $N_o{}^i$ was the number of events in the i^{th} bin, N^i was the fitted number of events in the i^{th} bin, and $\sigma_i{}^2$ was the variance of the number of events in the i^{th} bin. N^i was expressed as

$$N^i = \sum_{\ell=o}^{m} A_\ell P_\ell(x_i) \, \Delta x_i$$

where m is the order of the fit, $P_\ell(x_i)$ is the ℓ^{th} Legendre polynomial, A_ℓ is a scaler coefficient, and Δx_i is the width of the i^{th} bin. A Monte Carlo program was used to test STRAW by generating 450 histograms where each histogram was normalized to 600 events. Each histogram was generated by randomly choosing six coefficients and calculating

$$y(x) = \sum_{i=1}^{6} A_i P_i(x) \quad \text{for } -1 < x < 1 .$$

This curve was then partitioned into ten bins and the area of each bin was normalized such that the total area under the curve was 600. The area, A_i , of each bin was then varied with a gaussian distribution whose variance was $\sqrt{A_i}$.

A comparison was made of the coefficients determined by STRAW with the original coefficients used by the Monte Carlo program to generate the histograms. The difference between the fitted coefficients and the real coefficients was plotted to give an indication of the errors associated with the fit for Ao, which represents the total number of events in the fitted histogram; the errors were comparable to the error associated with the total number of events assuming a Poisson distribution. The errors on the other coefficients were of the same order of magnitude as those of Ao.

The data was initially plotted as two histograms of $d\sigma/d\Omega$ versus $\cos \theta^*$ for incident pion momenta of .893 and 1.03 BeV/c. $d\sigma/d\Omega$ was normalized to account for the beam contamination, scanning efficiency, spark chamber efficiencies, and geometrical biases. The inefficiency of the beam counters did not affect the normalization since the beam coincidence is independent of the final state of the beam particle. The beam counters can affect the normalization, however, by accidental counts, i.e., indicating a coincidence when there was not one. The accidental counting rate for the beam counters was calculated using the shortest spill time and maximum beam flux used during the experiment. The maximum calculated accidental rate was .15% of the average rate. The total beam contamination was 34% ± 2.9% and the total scanning efficiency was 98%. 10% ± 1% of all tracks in spark chamber 5 were outside the field of view of the field lenses and consequently were not photographed.

The plot of $d\sigma/d\Omega$ versus $\cos \theta^*$ corrected for beam contamination, optical rejections, and scanning efficiencies at the incident pion

momenta of .893 BeV/c was used to determine the spark chamber triggering efficiency as a function of the ionizing particles' angle from the beam direction and to determine the geometrical bias. 25% ± 5% of the $\pi^- + p$ elastic scattering events satisfying the logic requirements for elastic scattering events had one of the scattered particles intercept the outer aluminum jacket of the hydrogen wall. Since the probability of this occurring was a function of $\cos \theta^*$ as well as of the interaction point, this was considered a geometrical bias. The expected curve of $d\sigma/d\Omega$ versus $\cos \theta^*$ calculated with the phase shifts of Bareyre, et al.,[6] was plotted with the experimental histogram obtained from our experiment; this is illustrated in Figure 5. Bareyre's curve agreed quite well with the experimental histogram of Bertanza, et al., obtained at 900 MeV/c.[7] The .893 BeV/c data was used to determine these efficiencies since the known plot of $d\sigma/d\Omega$ versus $\cos \theta^*$ is smoothly decreasing over the experimental range of $\cos \theta^*$. This is not the case for the 1.03 BeV/c data.

The spark chamber efficiency for large angle tracks was determined by examining those events whose interaction occurred in the last half of the target. Events in this region had no geometrical biases. The corrections necessary to make the plot of $d\sigma/d\Omega$ versus $\cos \theta^*$ for this data agree with the histogram of Bareyre's data determined the spark chamber triggering efficiency as a function of the ionizing particles' angle. For angles less than 50° there was no detectable change in the spark chamber efficiencies within the experimental errors.

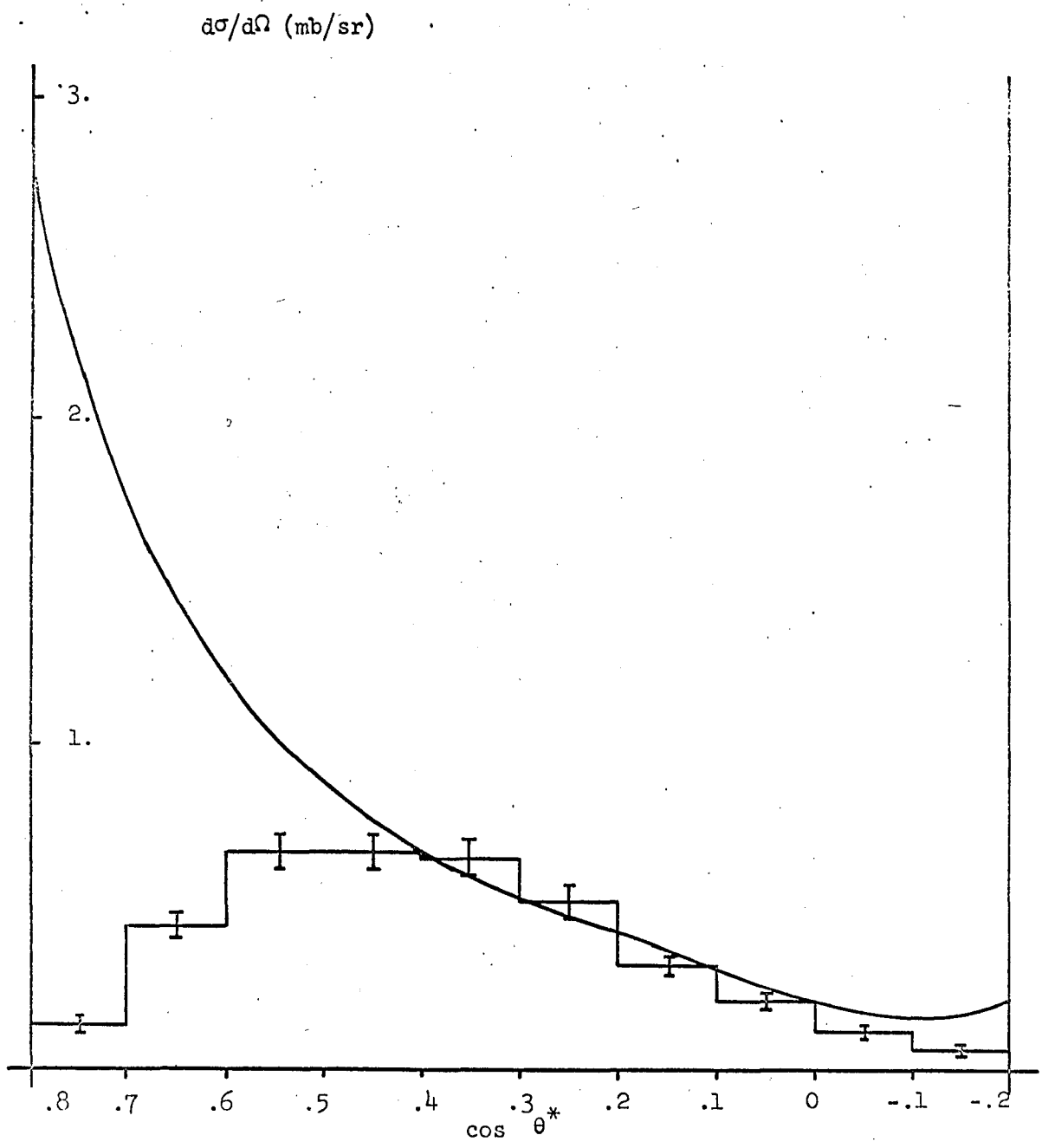

FIGURE 5 dσ/dΩ AT .893 BeV/c

The solid curve represents the data of Bareyre, et al. Our data shown is uncorrected for geometrical biases and for spark chamber angular efficiencies.

The spark chamber angular correction was then applied to all of the .893 BeV/c data to determine the geometrical biases. The corrections necessary for the .893 BeV/c to agree with that of Bareyre determined the geometrical biases.

30% of all elastic scattering events found by the scanners came from the region of the Λ° K° experiment scintillator, located .2" downstream from the hydrogen target. Since it is possible to kinematically identify $\pi^- p$ scatters on free protons in the scintillator, it is possible to include these events in our data. The validity of this was determined by separately plotting the coplanaraties of the target and of the scintillator events from a portion of the data. The graphs should show an elastic scattering peak over a smooth background, and both graphs, when the coplanarities of the fitted elastic scattering events were removed, indicated that this indeed occurred. This is illustrated in Figure 6.

Since the final analysis of the data requires accurately knowing the incident pion momentum, two more corrections to the $d\sigma/d\Omega$ are required. The first correction was due to the efficiency of the momentum spectrometer which was 65%. The second correction concerns the beam profile, i.e., the plot of the number of beam events versus beam momentum which is shown in Figure 2. The total incident flux measured at any momentum has a 2% half-width at half-maximum for our experimental setup. Consequently, when the events are grouped in momentum bins whose widths are smaller than 2% of the central momentum, the beam profile is needed to determine the incident flux for each bin.

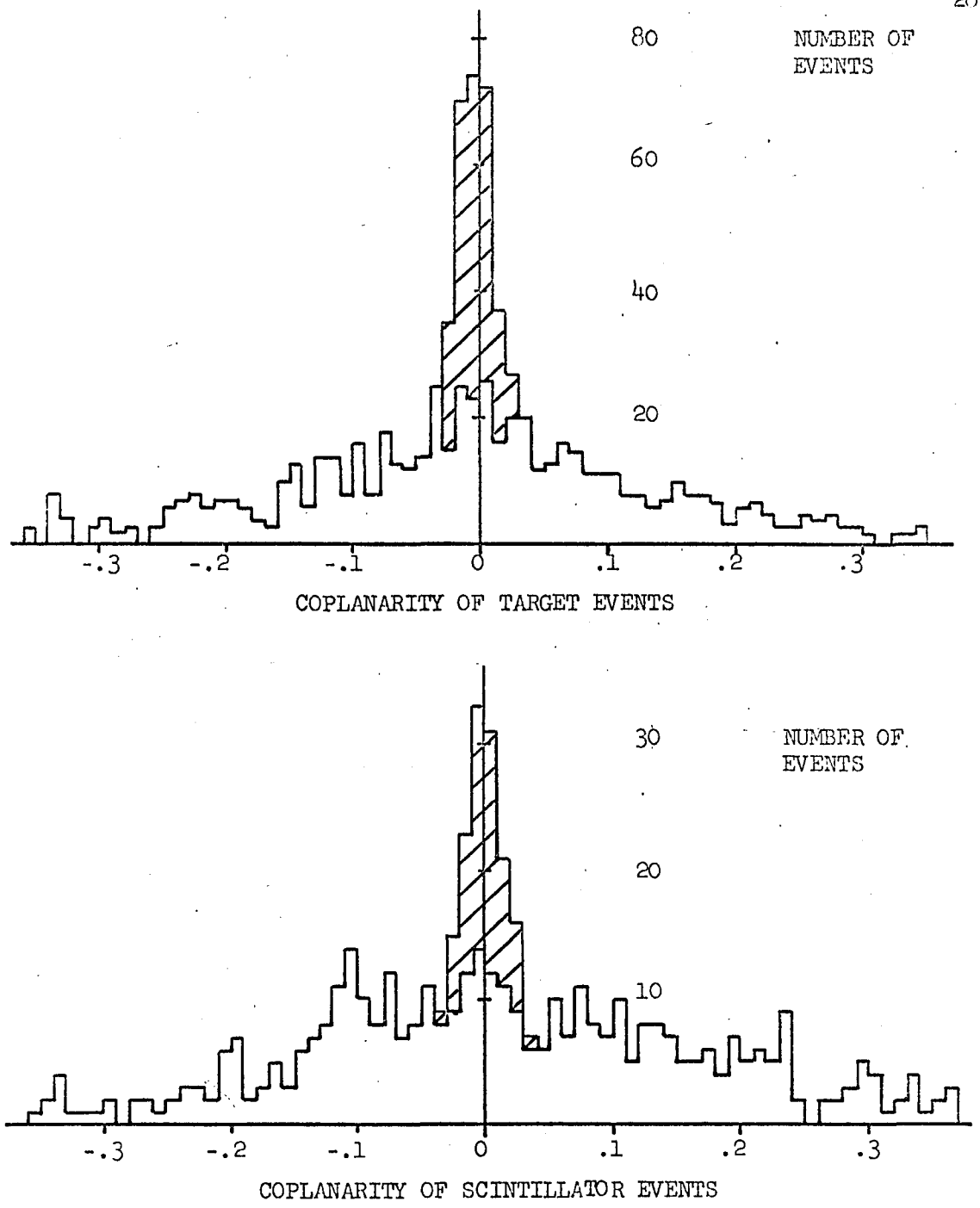

FIGURE 6 COPLANARITY OF TARGET AND SCINTILLATOR EVENTS

The shaded area represents the coplanarities of the events that satisfied the $\pi^- + p$ elastic fit.

The 1.03 BeV/c data was grouped into five momentum bins that were adjusted so that each bin represented the same number of incident pions. The accuracy of the beam profile was such that there was an 8% uncertainty of the incident pion flux in each bin. This was negligible compared to the 19% uncertainty in the number of π^- +p elastic scattering events in each bin.

4. RESULTS

The determination of the maximum Legendre polynomial needed to fit the data was made by examining the goodness-of-fit parameter $G = \chi^2/d$, where d is the number of degrees of freedom and χ^2 is the chi-square of the fit. The number of degrees of freedom is equal to the number of points fitted minus the order of the fit minus one. The goodness-of-fit parameter will decrease and level off as the order of the fit is increased. At the point where G becomes relatively constant, the minimum order of fit for statistical significance can be obtained. Our experimental fitting was done to a sixth order fit, even though a fifth order was sufficient.

The nominal 1.03 BeV/c histogram was fit to an orthogonal series of Legendre polynomials by STRAW, and its coefficients compared with the coefficients from similarly fitted histograms obtained by Duke, et al., over the angular range observed by our experiment.[8] The incident pion momenta of that data ranged from .875 to 1.28 BeV/c with a momentum spread of 2% (half width at half maximum). A plot was made of the ratio of the coefficients divided by the coefficients of the zero-th Legendre polynomial versus incident pion momentum. Our coefficients for 1.03 BeV/c with the 2% momentum spread agreed quite well with the Duke data. The corrected 1.03 BeV/c data is compared with that of Duke in Figure 7.

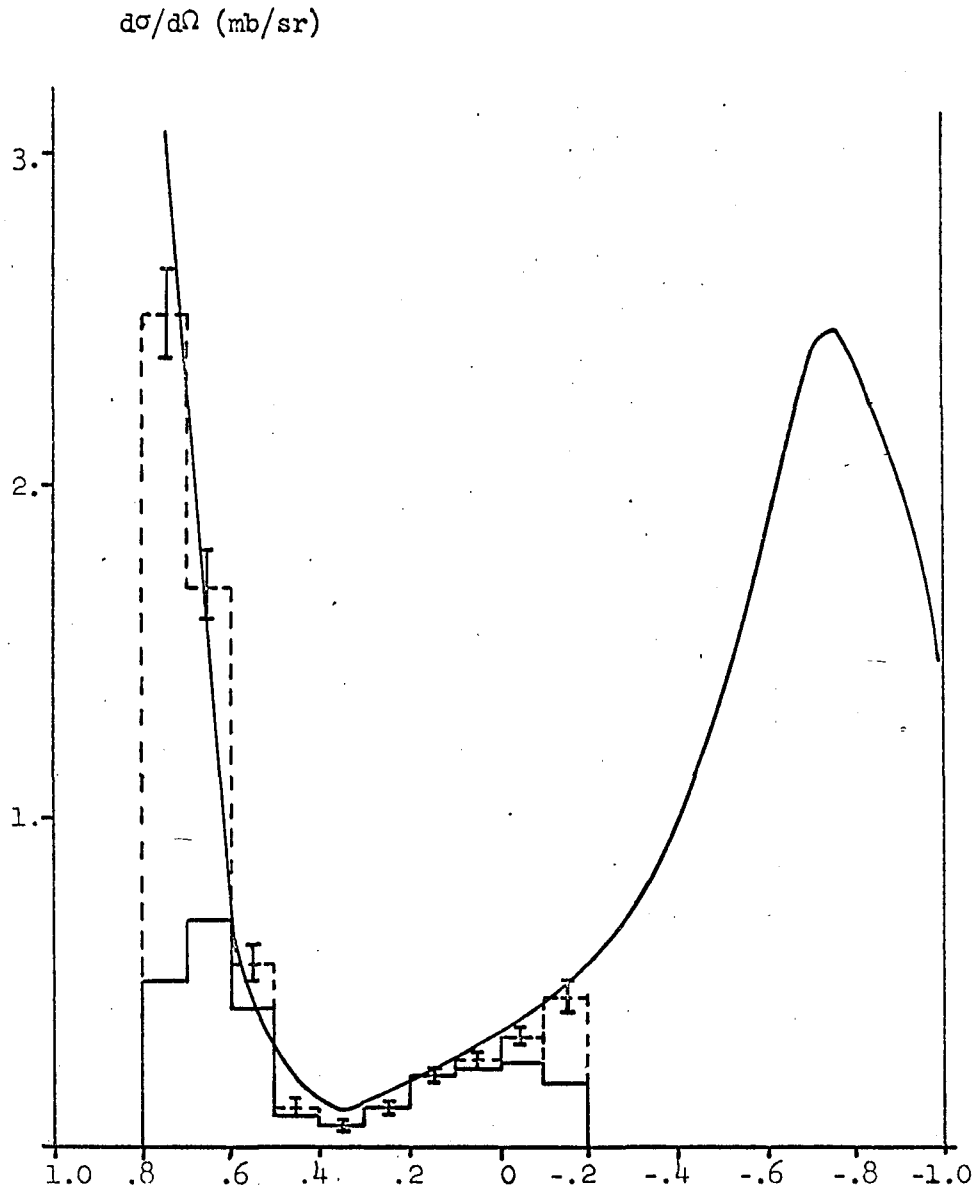

FIGURE 7 dσ/dΩ AT 1.03 BeV/c

The solid histogram represents our uncorrected data. The dashed histogram shows the corrected data. The solid curve is the data of Duke.

The nominal 1.03 BeV/c data is shown in Figure 8 as a histogram of five momentum bins, each of which contains only those events where $.05 < \cos \theta^* < .45$. This region is significant because here there is a large amount of destructive interference from the partial waves, which means that a rapid fluctuation with energy in a partial wave phase should be more apparent than in other regions. This region also does not require a correction due to the spark chamber angular efficiencies or the geometrical biases. The bin widths correspond to slices of equal incident flux.

This histogram was fitted to a straight line to ascertain whether any fluctuations could be observed due to a change in the momentum. A satisfactory fit to the partial cross-section, y, was $y = \alpha p + \beta$ where p was the incident momentum. The fit was a 3 constraint fit with a chi-squared of 1.8 and determined that $\alpha = 1.22 \pm .06$ (mb/st · BeV/c), $\beta = 1.42 \pm .06$ mb/st, and that, within the errors of this experiment, no fluctuations were present.

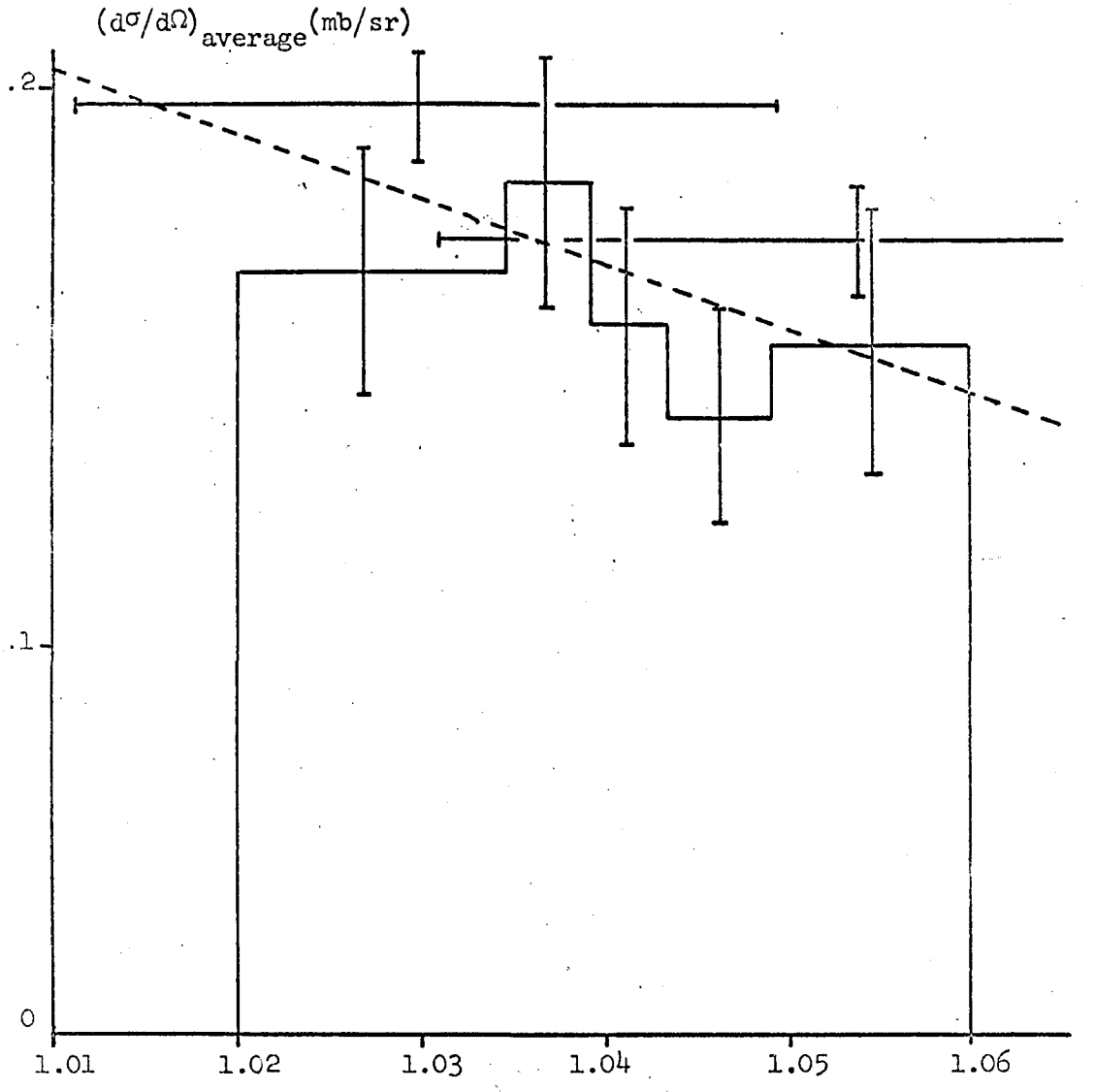

FIGURE 8 HISTOGRAM OF 1.03 BeV/c EVENTS FOR $.05 < \cos\theta^* < .45$

The histogram represents our data and the dashed line is our fit. The two points are from the data of Duke.

5. CONCLUSIONS

In order to visualize the conditions necessary for observing the Ericson fluctuations, consider the analogy of a wave guide and a closed cavity. Assume the cavity has a diameter L, and the incident wave has a wave length λ . If the cavity has a hole, allowing the wave to escape, the number of wave reflections before escape, n, can be written as $n = \frac{\hbar c}{\Gamma L}$, where Γ is the decay width of the system. The number of effective wavelengths in the box, ν, can be expressed as $\nu = \frac{nL}{\lambda} = \frac{\hbar c}{\Gamma \lambda}$. The fluctuations should occur if ν is changed by the order of unity since this will significantly change the phase of the scattered amplitude. This condition can be expressed either as

$$\delta\nu = \frac{\hbar c}{\Gamma \lambda^2}\delta\lambda \approx 1 \quad \text{or as} \quad \delta\lambda \approx \lambda/\nu \ .$$

Since the energy of the incident wave packet is $E = \frac{\hbar c}{\lambda}$, we can write $\nu = \frac{E}{\Gamma}$, and $\delta\nu \approx 1$ is then equivalent to $\delta E \approx \Gamma$.

It is possible to find fluctuations by examining a final state of a reaction at various energies or by examining the angular distribution. The criterion for observation of the fluctuations in an angular distribution is an angular resolution smaller than the width of the angular structure. The width of the angular structure is associated with ℓ_m, the maximum angular momentum contributing to the reaction. Since the greatest complexity of an angular distribution is $\cos^{2\ell_m}\theta$, we note that at 1.03 BeV/c this width is approximately 25°, which means that at this energy it is unreasonable to observe the fluctuations in angular distributions. Our

experiment therefore examined π^- +p elastic scattering final state at various energies.

If the typical width of the energy structure for the pion-proton system were of the order of the pion mass, then Ericson fluctuations would have been observed previously in high energy pion-proton experiments. Although the pion mass is generally considered to be the strong interaction width, one can consider the widths of various pion-nucleon systems as well as the width of the nucleon. These widths range over many orders of magnitude, and consequently it is not too unreasonable to expect that there might be states of the pion-nucleon system whose widths would be on the order of 1 Mev. If such states existed in the region of 1.02 - 1.06 BeV/c, then our experiment could have observed possible Ericson fluctuations.

Our failure to observe the fluctuations can be attributed to one of three possibilities. It is possible that there are characteristic widths of the pion-nucleon system considerably narrower than 1 MeV/c. In this case, the fluctuations would not be observed because our experimental resolution was not good enough. The second possibility is that the Ericson fluctuations do not occur in high energy pion-nucleon processes at our energy. Finally, it is possible that the assumption of a random distribution of the matrix elements is invalid and that there is a correlation between the partial waves; this means that Ericson fluctuations would not occur at any energy for elementary particle collisions. This would agree with the conclusion of Allaby, et al., who investigated the fluctuations in the angular distribution of proton-proton scattering at 16.9 BeV/c.[3]

REFERENCES

1. T. Ericson, Physical Review Letters 5, 430 (1960).

2. T. Ericson and T. Mayer-Kuckuk, Annual Review of Nuclear Science 16, 183 (1966).

3. J. Allaby, G. Bellettini, G. Cocconi, A. Diddens, M Good, G. Matthiae, E. Scaharidis, A. Silverman, and A. Wetherell, Physics Letters 23, 389 (1966).

4. G. Abrams, University of Maryland Technical Report No. 720 (1967) unpublished.

5. R. Böch, CERN Report 64-13 (1964).

6. P. Bareyre, C. Brickman, A. Stirling, and G. Villet, Physics Letters 18, 342 (1965).

7. L. Bertanza, A. Bigi, R. Carrara, and R. Casali, Nuovo Cimento 44, 712 (1966).

8. P. Duke, D. Jones, M. Kemp, P Murphy, J. Prentice, J. Thersher, and H. Atkinson, Physical Review Letters 15, 468 (1965).